Experimental Investigation of Mechanical Performance of Basalt/Epoxy/MWCNT/SiC Reinforced Hybrid Fiber Metal Laminates

Shanmugaselvam Palaniyandi[a], Dhinakaran Veeman[a]*

[a]Centre for Additive Manufacturing, Chennai Institute of Technology, 600069, Chennai, India.

The primary goal of this study is to see how multi-walled carbon nano tubes (MWCNTs) and nano silicon carbide particles (SiC) affect basalt reinforced epoxy composites made using pressure mould. The aluminium 8090 metal plate was used to strengthen the laminate's core. Tensile, bending, and low velocity impact tests, as well as aesthetics, were investigated and presented for the debate. The physical and low velocity impact characteristics of the produced laminates are considerably improved by including MWCNT/SiC into the epoxy matrix and basalt mixture. The 9 wt. % and 12 wt. % of SiC filled combinations show higher tensile and flexural performances up to 40% than neat composites among the investigated combinations. Drop weight impact tests show a progressive improved energy absorbing response of up to 60% as SiC reinforcement increases. SEM morphology of pure, SiC/MWCNT filled specimens, as well as fragmented surface analyses, were also presented. It was observed from morphological studies that there is a reasonable wettability between matrix/filler/reinforcements. This research work will lay a path for using Basalt/Epoxy/MWCNT/SiC Reinforced Hybrid Fiber Metal Laminates for aerospace and structural applications.

Keywords: *Basalt fiber, Epoxy matrix, hybrid composite, Fiber metal laminates, Multi-walled carbon, nano tubes, Silicon carbide, SEM.*

1. Introduction

Four decades earlier, the emergence of polymer nano composites ushered a new era in the fiercely competitive, material-intensive sector of aeroplane construction[1]. Fiber-reinforced composite materials, with their primary properties of high specific strength and stiffness, have already been contending for a share of aeroplane body over time. However, their own achievement has indeed been confronted with a number of relatively insignificant downsides in contrast to aluminium, such as formability, processability, weldability, inspectability, maintainability, shock resistance, notch sensitivity, sturdiness, and price[2-4]. In the thick of the battle involving composite alloys and resin matrix composites, a new contender appears to have just joined the fray: a new breed of materials (See Figure 1) known as Fiber Metal Laminates (FML)[5].

The poor durability of polymer fiber composites has led to the development of fiber metal laminates (FMLs). GLARE® composites have become the most well-known laminates with the most widespread commercial use[6]. Polymeric composite materials, which absorb the energy via matrix and fiber fracturing[7-9], whereas GLARE® and other types of FMLs[10,11] absorb the energy primarily by plastic strain of plates. Numerous researchers attempted Polymer matrix Fiber Metal laminates to develop advanced high strength composites for industrial applications. Bahari-Sambran et al.[12] studied the mechanical characteristics of basalt/epoxy fiber metal laminates with varying weight

percentages of nano clay. The results showed a considerable increase in impact energy absorption behavior, with up to 40% improvement in the results.

Yamada et al.[13] found that introducing a metallic strip at the bi-material boundary with aluminium and fibrous composite could reduce fiber rupture. Several research firms, academia, and the aerospace industry have looked into the mechanical characteristics of FML. Kazemi-Khasragh et al[14]. investigated the effect of different graphene nano-platelets (GNPs) content on the tensile, flexural, and Charpy impact characteristics of carbon, Kevlar, and hybrid carbon/Kevlar fibers reinforced epoxy matrix composites and found that GNPs particle content up to 0.1 and 0.25 wt percent have better flexibility than similar grade materials.

The key tests used to screen the qualities of FML are tension, impact, fatigue, shear and compression tension, compression[15-18]. The mechanical behavior CNTs nano - composites having epoxy matrix was studied by Zhou et al.[19]. They found a rising pattern in composite elasticity as a function of CNT addition, while flexural modulus declined at improved wt. % of CNTs up to 10 wt. %. The increase in strength and flexural modulus at lower CNT loadings was related to the limitation of the polymeric strands movement, according to the researchers. Kostopoulos et al.[20] investigated the impact behavior of MWCNTs/CFRP nano composites at various impact energy levels. The inclusion of CNTs had no effect on the impact behavior of composites, according to their findings.

Santhosh et al[21]. investigated fire performance of glass reinforced phenolic/APP composites and reported
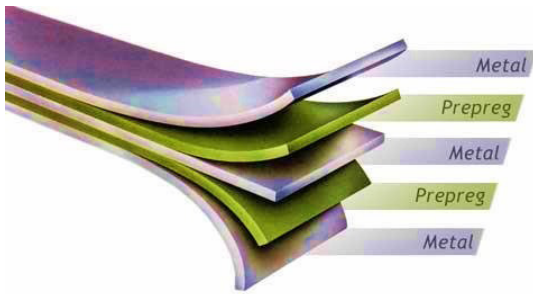
*e-mail: dhinakaranv@citchennai.net

Figure 1. Schematic illustration of fiber metal laminates.

it's mechanical and fire behaviors. It was found from the results that there is a significant improvement in the fire performance and tensile behavior on resultant composites due to the inclusion of ammonium polyphosphate fillers up to 10 wt. % and starts to shrink with further more addition of APP. Rahman et al.[22] investigated the higher intensity behavior of amino-functionalized multi-walled CNTs (NH_2-MWCNTs) reinforced E-glass/epoxy composites in a similar research. The use of 0.3 wt. % NH_2-MWCNTs enhanced the absorbed energy, limit velocity, and damage area values of composites when compared to neat composites. The inclusion of MWCNTs at 0.5 wt. %, on the other hand, had a negative influence on the composites' high-velocity impact behavior. MWCNTs had a detrimental impact at 0.5 wt. % addition due to the agglomeration and higher resin fluidity.

Nakatani et al.[23] investigated the degradation of titanium/GFRP hybrid composites during ballistic impact and determined that the fracturing dominates the impact behavior of the titanium/GFRP laminates on the quasi side, in the titanium layer. Li et al.[24] investigated the dynamic performance of Ti/CFRP/Ti composites with various titanium strip surface modifications, including tempering, sandblasting, and electroplating. When the metal surfaces were sandblasted and anodized, the durability of the metal alloy interaction was significantly increased compared to when the titanium plates were left unprocessed. Tarfaoui et al.[25] investigated the tensile characteristics of polymer composites using varying volume fractions of carbon nanotubes. The inclusion of CNTs resulted in a loss of mechanical characteristics, according to their findings. Furthermore, CNTs had no influence on stiffness levels, according to the researchers. Nano particles inclusion into the matrix of fiber metal laminates greatly improves its behavior from the micro constituent's level[26].

Numerous studies have been documented the influence of stacking sequence, fiber orientation, matrix characteristics, and aluminium surface finishes on mechanical and morphological behavior of different fiber materials, according to the aforementioned literatures. While there is a significant research gap in the low velocity impact behavior study, the influence of SiC and multi wall carbon nanotubes incorporation on the mechanical behavior of basalt/Aluminum laminates. The current study investigates fiber metal laminates reinforced with Basalt/Aluminium sheet/SiC and MWCNT in various proportions to pick the optimum filler ratio for advanced composite structure replacements such as boat hulls, aerospace panels, and structural engineering components.

2. Experimental Procedures

2.1. Materials and fabrication of samples

FMLs are constructed using basalt fibre and aluminium 8090 metal plates in this study. Hindustan composites ltd, Maharashtra, provided the basalt fibers. Aishwarya polymers, Coimbatore, Tamilnadu, provided the epoxy coating matrix LY 556 (density 0.9 g/cm³, viscosity 1.25x104 cP) and hardener W152 LR (density 1.2 g/cm³, viscosity 1.30x104 cP). Nanocyl, Belgium, provided MWCNT from the NANOCYL® NC7000TM line. The provider produces MWCNTs as thin tube-shaped materials using the Catalytic Chemical Vapour Deposition (CCVD) technique. The tubular has an average size of 9.5 nm, a length of 100 m, and a density of 1.3 g/cm³. Nano silica particles with the average size of 140 nm were supplied by the Nanoshell, Maharashtra. Tables 1, 2 and Figure 2 shows the parameters of reinforcing fibers, matrix materials, aluminium alloy plates and image of MWCNTS respectively, as specified by the supplier.

Aluminum AA8090 boards with a surface area of 1mm (containing 95.2 percent Al, 0.36 percent Fe, 0.02 percent Ti, 3.83 percent Mg, 0.23 percent Mn, 0.17 percent Si, 0.01 percent Zn, 0.01 percent Cu, and 0.15 percent Cr), bidirectional basalt fibre (E-glass 450 g/m²), and epoxy resin were used to make the specimens (Huntsman, LY 556 with hardener HY 5160). Schematic illustration of the developed FML laminates was depicted in Figure 3.

The open lay-up approach was used to create the specimens, which were then pressurized throughout the healing phase. As a byproduct of the pressurization, voids are reduced and superfluous glue is removed. Residual voids were quite tiny and hence unnoticed. In basalt/epoxy layers, the mean volume percentage of fibers was 57 percent, with tertiary reinforcement percentages varying.

The basalt matrix fiber accounted for over 65 percent of the total weight. To establish strong relation between fiber and Al panels, basalt fibers were alkaline pre-treated and the surface of aluminium sheets were grooved inversely. Six groups of symmetric specimens with different weight percentages of MWCNT (0.5, 1, 1.5, 2, 2.5 wt. percent) and Nan silica (3, 6, 9, 12, 15 wt. percent) were fabricated, and the investigational results have been compared to the filler-unreinforced setups to determine the best filler proportion for resilience and mechanical characteristics. Schematic illustration of the FML laminates developed for the flexural and low velocity impact tests were depicted in Figure 3. Similarly Table 3 shows the annotations, filler proportions, and specimens for each. In each configurations three samples were prepared for the characterizations as per ASTM standards and its average values are reported for the discussions.

2.2. Mechanical testing and characterization

Most of the tests have been carried out in a National Accreditation Board for Labs (NABL) accredited, Indian Institute of Technology - Madras and a National Accreditation Board for Certification Bodies (NABCB) accredited National Labs in Chennai, Tamil Nadu, India, in accordance with ASTM Norms. Tensile tests according to ASTM D3039 in a universal tensile testing machine (Instron 8801 with 150 kN

Table 1. Properties of core aluminium, fiber and resin matrix.

Property/Grade	Basalt	Epoxy Matrix	Al 8090
Density (g/cm^3)	2.67 g/cm^3	1.15	2.70
Tensile strength (MPa)	1450-2500	80–95	420
Tensile modulus (GPa)	75-87	0.3–0.6	70.05
Grade (GSM)	450	-	500
Elongation at break (%)	2.8-3.5	-	-
Color	-	Pale Yellow	-
Yield Strength (MPa)	-	-	315
Fatigue Strength (MPa)	-	-	105.6
Poisson ratio	-	-	0.33

Figure 2. Multiwalled Carbon Nanotubes (scale: 100 nm – TEM).

Table 2. Properties of Secondary reinforcements.

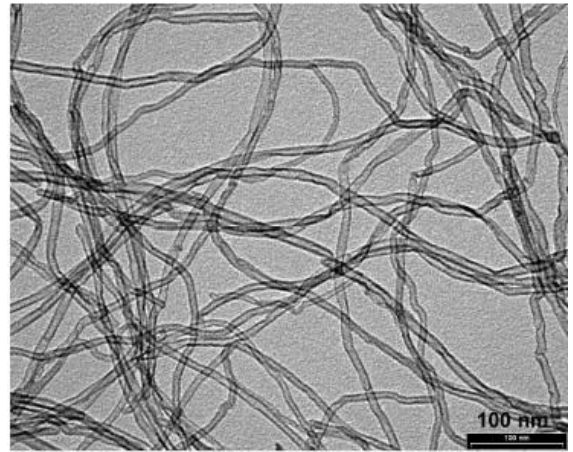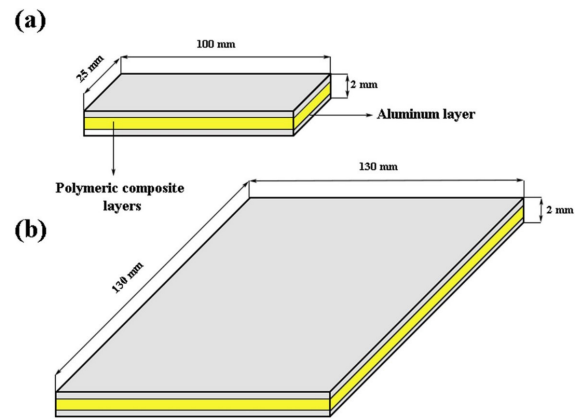| Property/Grade	MWCNT	Nano SiC
Purity (wt. %)	99.5	99.8
Thickness (nm)	4-20	-
Average size (μm)	9.5	140
Length (m)	100	-
Density (g/cm^3)	1.3	4.4
Surface specific area (m^2/g)	174	202

Table 3. Notations of hybrid laminates developed for the investigations.

Specimen Code	Configuration of hybrid fiber laminate
NFML	Basalt + Al 8090
HFML1	Basalt + Al 8090 + 0.5 wt. % MWCNT + 3 wt. % Nano SiC
HFML2	Basalt + Al 8090 + 1 wt. % MWCNT + 6 wt. % Nano SiC
HFML3	Basalt + Al 8090 + 1.5 wt. % MWCNT + 9 wt. % Nano SiC
HFML4	Basalt + Al 8090 + 2 wt. % MWCNT + 12 wt. % Nano SiC
HFML5	Basalt + Al 8090 + 2.5 wt. % MWCNT + 15 wt. % Nano SiC

*HFML – Hybrid Fiber metal Laminate

Figure 3. Illustration of the FML samples.

load cell) at ambient temperature (23 C, 50% moisture). To retain the item and preventing it from sliding and breaking at the grip location, a wedge style grip was utilized. Load was progressively applied to the material at a cross - head depth of 5 mm/min, and the file's data were recorded, including tensile strength, elastic strength, and failure strain. Each wt. % had five samples analyzed, with the average of the findings determined and taken into account.

It is critical to investigate the polymeric composite's abrupt impact behavior since it is frequently used in unintentional accidents. As a result, Izod impact specimens were developed in accordance with ASTM D256. The damage test was conducted using an AIT-300N impact tester with a pendulum swing of 1800 mm and a striking hammer weight of 16.5 kg. 1.25 kg weight was used in IFW (Falling weight impact) testing with a samples of 100 mm x 100 mm – ASTM D7136/D7136M-15 norm. The device's higher impact height ranges between 50 to 6000 mm, and the test was conducted with a d90 kind of nose. IFW tests were performed using a constant mass of 1.25 kg and altering the falling height.

2.3. XRD and SEM Analysis

In attempt to comprehend the level of distribution of SiC and MWCNT nano particles in matrix, XRD assessment was conducted on specimens for weight fractions of nanosilica. XRD Machine (Bruker D8, Karlsruhe, Bruker AXS GmbH, Germany) powered at 40 kV, 40 mA, and a screening rate of 2/min was used to evaluate the samples. Bragg's law was used to calculate the crystallography space (d-spacing). The changed quantities of parallelization were used to assess the nano layered material (gently exfoliate).

Likewise the morphology and degradation mechanisms of the materials were studied using scanning electron microscopy (SEM). The infinitesimal image of the unfractured and fractured specimens was captured using an FEI Quanta 400F Field Emission microscope (up to 100 000 000,00x magnification) with an applied potential of 0.5 – 45 kV, a

highest image recognition precision of 3584 x 3094 pixel, and a thermoelectric energy dispersive gun. Microscopic photographs of cracked surface and unfractured samples were collected and reviewed in depth at various magnifications and orientations.

3. Results and Discussions

3.1. XRD Analysis

In terms of lattice spacing, filler distribution in substrate may indeed be classified both as intercalated and desorbed. When the diffusion length (d-spacing) is more than 10 nm, the dispersal behavior is characterized as graphitic[27]. Figure 4 shows the X - ray diffraction pattern of true and nano silica reinforced composite structures. In Diffraction, the level of nano - silica distribution in the matrix was clearly visible.

The clean epoxy had a strong peak at 18.99^0 with a steep slope, while the 1, 2, and 3 wt. % of nanosilica reinforced materials had peaks at 18.55^0, 18.59^0, and 18.97^0, correspondingly. Because of the micro porous form, very faint peaks were identified in the instance of 3 wt. % nanosilica. This might be owing to increased viscosity and slenderness of the substrate as the nano - silica concentration increased, resulting in poor distribution and aggregation.

3.2. SEM Analysis

Firstly morphology of the hybrid samples was captured using FESEM to analyze the matrix reinforcement bonding and filler disbursements. For the better clarification HFML1, HFML3 and HFML5 configurations were taken for the analysis and compared with the Neat laminates. The numerous strengthening processes in the MWCNT/SiC/Epoxy filled adhesive systems, which significantly impacts the FML's characteristics, are shown in Figure 5. The fracture spanning and breaking of MWCNTs are seen in Figure 5a. The incidence of fracture development is hampered by crack spanning. The existence of adhesive forces among MWCNTs and epoxy resin is also demonstrated by MWCNT perforating[28,29].

Some other identified process in MWCNTs squeeze, as seen in Figure 5b. The Nanostructures move away first from epoxy coating in Figure 5b and Figure 6c, suggesting the existence of a thermoplastic vacancy development process.
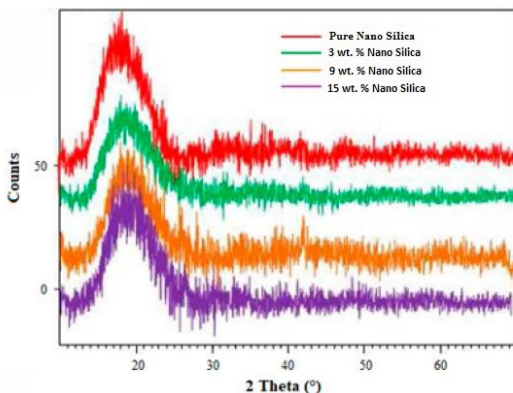

Figure 4. XRD Spectra of virgin and hybrid composites.

One of its key stiffening processes for composite samples CNTs is elastic gap expansion, which happens following nanoparticles delamination. In reality, as a result of brittle failure and consequent plastic void expansion, the absorption coefficient rises, increasing the mechanical characteristics of samples. However 5 (d) clearly evidences that still there is a harder or irregular surface on the neat specimen due to the matrix materials agglomeration.

3.3. Tensile behavior of the samples

Figure 6 shows the tension behavior of several weight percent filler reinforced hybrid samples. The tensile properties of the core supplement basalt are well known to be somewhat larger than those of other comparable class fibers. It was determined from the stress and strain relationship treatment that neat specimen NFML had a higher tensile strength of 243.037 MPa. The toughness of 3, 6, 9, 12, and 15 wt. percent nano silica ranges between 268.316 MPa, 281.152 MPa, 293.031 MPa, 239.431 MPa, and 226.302 MPa. Tensile strength improves up to 9 wt. percent fillers injection, then progressively falls for 12 and 15 wt. percent filler introduction. The strength of the 9 wt. percent SiC/MWCNT loaded specimen is 20.57 times better than that of the clean epoxy specimen.

Conversely, when the weight % of SiC rises, the elastic strength increases gradually. The elasticity of neat samples ranges from 44.62 GPa, 46.326 GPa, 47.815 GPa, 48.503 GPa, and 49.865 GPa for 3, 6, 9, 12, 15 wt. percent, correspondingly. The tensile modulus of HFML5 is 21.52 percent higher than that of plain lamination. The results showed that effective matrix-reinforcement interfacial bonding and homogeneous diffusion of SiC/MWCNT fillers into the matrix resulted in an improvement in tensile strength[27]. Tensile modulus gradually raises until the filler percentage improves and there is a significant raise in the breaking load capacity up to 9 wt. % filler percentage. Furthermore, toughness was limited resulting in an increase in matrix rigidity – filler ratios.

3.4. Flexural behavior of the samples

Four bending dynamic strength of produced hybrid specimens is shown in Figures 7a and b. The flexural strength of HFML3 (285.18 MPa) was found to be significantly higher than those of pristine composites. Flexural modulus falls significantly in HFML4 and HFML5. The strength of NAPP6 is 32.2 points greater than that of plain composite. The poor and improved interfacial bonding of matrix and reinforcing material causes higher tensile strength and limitation. The final goal is to find the moment when the filler loading rate begins to degrade, and the final goal is to find the phase where its filler loading percentage continues to diminish.

Hu et al.[30] described a similar scenario of bending breakdown deterioration in E-Glass hybrids with increased SiC load input. The elastic strength of comparably neat alloys is 13.491 GPa. Modulus values for 3, 6, 9, 12, and 15 weight percentages were 15.653 GPa, 16.051 GPa, 16.861 GPa, 17.932 GPa, and 19.162 GPa, correspondingly. To the equivalent load, a steady rise in the elastic strength was seen. The elasticity of HFML5 is 42.32 percent greater than that of tidy arrangement.
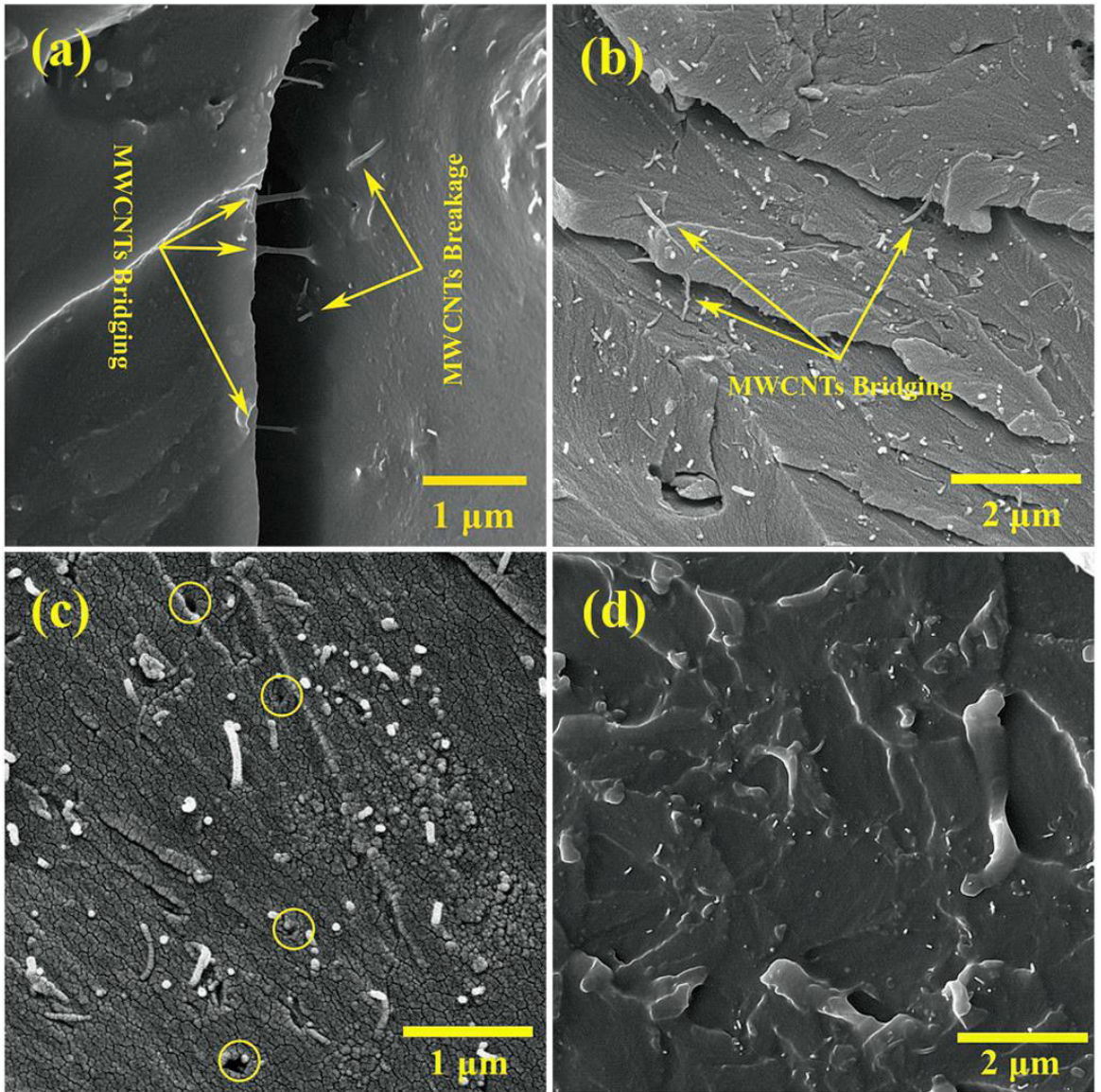
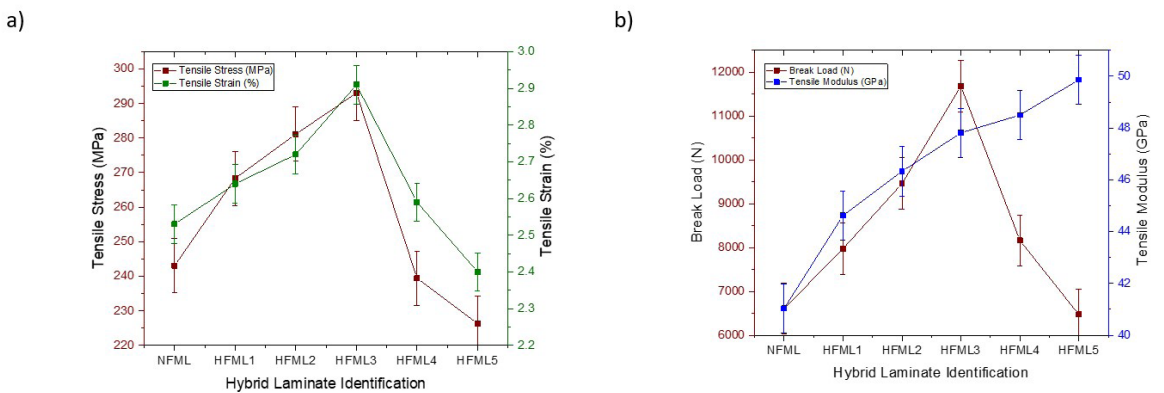**Figure 5.** Morphology of the hybrid fiber metal laminates.

Figure 6. (a) Stress-strain (b) Breaking Load - Tensile modulus behaviors of hybrid composites.
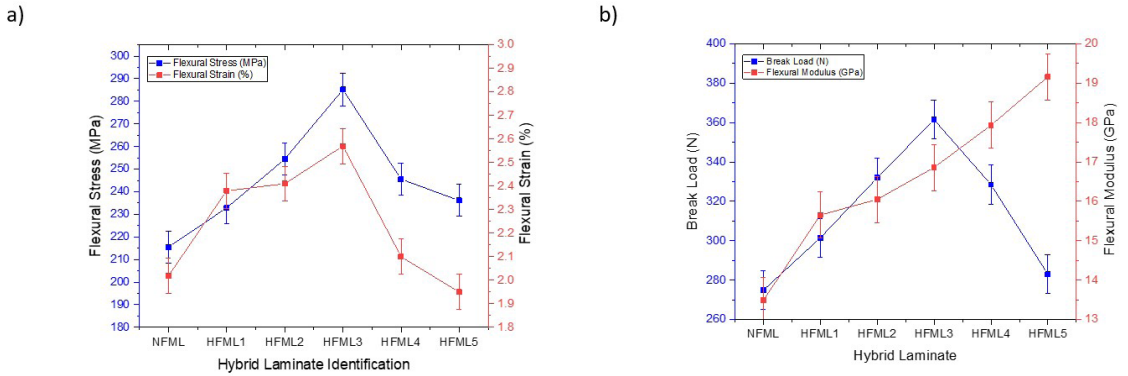
a)

b)

Figure 7. (a) Stress-strain (b) Breaking Load - Flexural modulus behaviors of hybrid composites.

3.5. IZOD and falling weight impact test

Figure 8 shows the Izod impact test results for hybrid systems. The findings of the Izod tests reveal that SiC/MWCNTs with more reinforcements can absorb more impact force. With the addition of fillers reinforcements, the load capacity of composites steadily rises. The HFML5 hybrid composite (Basalt + Al 8090 + 2.5 wt. % MWCNT + 15 wt% Nano SiC) has a higher energy uptake than other composites. It has been discovered that a hybrid design including 9 wt. percent SiC produces results that are closer to the maximum filler weight. The energy absorption capability of HFML5 is 54.3 percent greater than that of neat laminates. The incorporation of SiC/MWCNT considerably strengthens the matrix and improves the impact resistance behavior, according to the findings[31].

To examine the principles of specimen stabilization behavior, a falling weight impact test was planned to be performed on a moderately high impact energy absorbing nominee produced from izod impact testing. According to the izod test findings, HFML5 has greater energy absorbency. Figure 9 shows the falling weight test results of a 15 wt. percent SiC filled fabrication, which show that for different heights of loosing weight, such as 2 metres, 2.5 metres, 3 metres, 3.5 metres, and 4 metres, suitable energy uptake was achieved with a higher proportion of APP loaded configuration. The projected hybrid laminate recorded a peak power uptake of 62, 70, 80, 86, and 98 Joules.

3.6. Fracture analysis

Figure 10 shows fractured edges (tensile samples) of 9 wt. percent SiC loaded arrangement acquired using a scanning electron microscopy. The smooth and rough surface of the aggregate following breakage is shown in Figure 10a and c. The photos clearly show that there is good interfacial interaction among reinforcement materials in the clean surface area. Poor bonding occurs in slightly rough regions due to aggregation or a larger density of APP nanoparticles. Filler and matrix contacts play a vital role in the research of crystal lattice and fracture surface analysis, and they have a direct impact on the overall mechanical characteristics of hybrid laminates[30].

Diagram (b) displays the creation and spread of cracks in the matrices as the load is increased. The fibre is severely fractured near the conclusion of crack growth due to generated
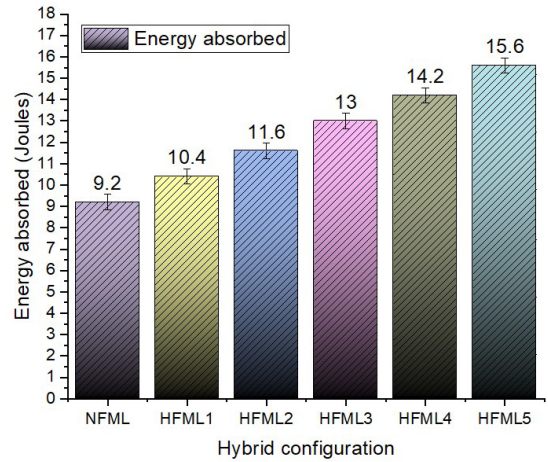
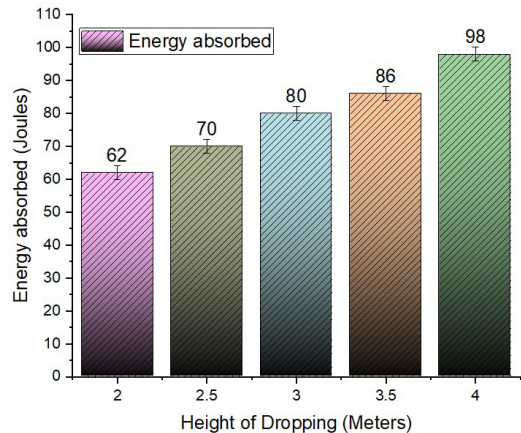**Figure 8.** Izod energy absorption capacity of neat and hybrid composites.

Figure 9. Drop impact capacity of neat and hybrid composites.

stress. Figures 10d and e depict fiber breakage and pull outs, respectively. Figure 10f demonstrates that, despite the fact that losses due to produced strain occur, there is a
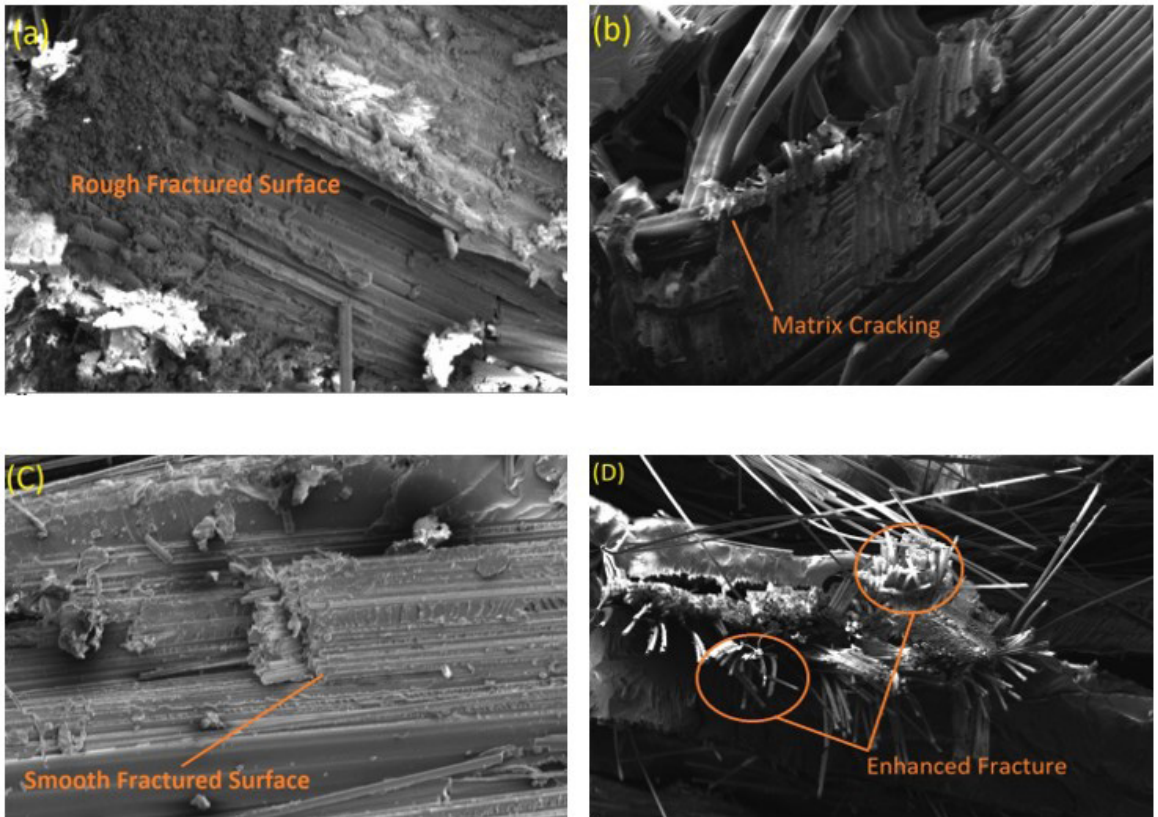
Figure 10. Failed surfaces of 9 wt. % SiC filled configuration (a) Rough fractured surfaces, (b) Matrix cracking and crack propagation, (c) Smooth matrix, (d) Fiber fracture zones, (e) Fiber pull outs, (f) Matrix fiber bonding.

strong bonding zone where the substrate, reinforcements, and fillers have a superior physical relationship. A good interfacial connection between matrix and reinforcement is seen in the smooth surface area. Poor bonding is found in the rough surface region due to agglomeration. In the samples where new cracks were produced before existing crack probation, the crack blowing process was also evident. In particle reinforced composite structures, these behaviours were widespread[32].

4. Conclusions

Using a compression molding process, a basalt/epoxy matrix loaded with varied amounts of MWCNT/SiC was created and observed results were pointed out below.

- The mechanical properties and geometry of both plain and SiC-modified samples, as well as shattered samples, were studied and described in depth.
- The strength of the 9 wt. % SiC (HFML3) filled structure is 293.031 MPa and 285.18 MPa, respectively, according to the tensile and flexural response measurements. This is greater by 20.57 percent and 32.2% over the pristine basalt/epoxy setup (NEAT).
- Low velocity impact tests, such as izod and drop impact tests, revealed a progressive rise in energy absorptions when the SiC/MWCNT filler % was increased.

- HFML5 has a 54.5% better energy retention than neat composites and is a good choice for shock workloads.
- In pristine compounds, SEM investigations reveal stronger fiber matrix interfacial adhesion, but in HFML3 and HFML4, bond formation is mild. SiC incorporation up to a specific level improves bonding and restricts bonding when it surpasses 12 wt. %.
- According to the results of the experiments, NAPP6 has superior flexural and tensile characteristics.
- The proposed research prepared the path for selecting possible candidates for creating aerospace structural applications, as well as conducting and reporting all essential trials.

5. References

1. He W, Wang L, Liu H, Wang C, Yao L, Li Q, et al. On impact behavior of fiber metal laminate (FML) structures: a state-of-the-art review. Thin-walled Struct. 2021;167:108026.
2. Droździel M, Jakubczak P, Bieniaś J. Low-velocity impact resistance of thin-ply in comparison with conventional aluminium-carbon laminates. Compos Struct. 2021;256:113083.
3. Jakubczak P, Podolak P. The issue of CAI assessment of fiber metal laminates. Compos Struct. 2022;281:114959.
4. Sinmazçelik T, Avcu E, Bora MO, Coban O. A review: fibre metal laminates, background, bonding types and applied test methods. Mater Des. 2011;32(7):3671-85.

5. Jakubczak P, Bieniaś J. The response of hybrid titanium carbon laminates to the low-velocity impact. Eng Fract Mech. 2021;246:107608.

6. Artero-Guerrero JA, Pernas-Sánchez J, Martín-Montal J, Varas D, López-Puente J. The influence of laminate stacking sequence on ballistic limit using a combined experimental/FEM/Artificial Neural Networks (ANN) methodology. Compos Struct. 2018;183:299-308.

7. Koziol M. Evaluation of classic and 3D glass fiber reinforced polymer laminates through circular support drop weight tests. Compos, Part B Eng. 2019;168:561-71.

8. Jakubczak P. The impact behavior of hybrid titanium glass laminates: experimental and numerical approach. Int J Mech Sci. 2019;159:58-73.

9. Pernas-Sánchez J, Artero-Guerrero JA, Varas D, López-Puente J. Experimental analysis of ice sphere impacts on unidirectional carbon/epoxy laminates. Int J Impact Eng. 2016;96:1-10.

10. Jakubczak P, Bieniaś J, Dadej K. Experimental and numerical investigation into the impact resistance of aluminium carbon laminates. Compos Struct. 2020;244:112319.

11. Jakubczak P, Bieniaś J, Droździel M. The collation of impact behaviour of titanium/carbon, aluminum/carbon and conventional carbon fibres laminates. Thin-walled Struct. 2020;155:106952.

12. Bahari-Sambran F, Meuchelboeck J, Kazemi-Khasragh E, Eslami-Farsani R, Arbab Chirani S. The effect of surface modified nano clay on the interfacial and mechanical properties of basalt fiber metal laminates. Thin-walled Struct. 2019;144:106343.

13. Yamada K, Kötter B, Nishikawa M, Fukudome S, Matsuda N, Kawabe K, et al. Mechanical properties and failure mode of thin-ply fiber metal laminates under out-of-plane loading. Compos, Part A Appl Sci Manuf. 2021;143:106267.

14. Kazemi-Khasragh E, Bahari-Sambran F, Siadati SMH, Eslami-Farsani R, Arbab Chirani S. The effects of surface-modified graphene nano platelets on the sliding wear properties of basalt fibers-reinforced epoxy composites. J Appl Polym Sci. 2019;136(39):47986.

15. Botelho EC, Almeida RS, Pardini LC, Rezende MC. Influence of hygrothermal conditioning on the elastic properties of carall laminates. Appl Compos Mater. 2007;14(3):209-22.

16. He W, Wang L, Liu H, Wang C, Yao L, Li Q, et al. On impact behavior of fiber metal laminate (FML) structures: a state-of-the-art review. Thin-walled Struct. 2021;167:108026.

17. Yao L, Zhang S, Cao X, Gu Z, Wang C, He W. Tensile mechanical behavior and failure mechanisms of fiber metal laminates under various temperature environments. Compos Struct. 2022;284:115142.

18. Bertolini R, Savio E, Ghiotti A, Bruschi S. The effect of cryogenic cooling and drill bit on the hole quality when drilling magnesium-based fiber metal laminates. Procedia Manufacturing. 2021;53:118-27.

19. Zhou Y, Pervin F, Lewis L, Jeelani S. Experimental study on the thermal and mechanical properties of multi-walled carbon nanotube-reinforced epoxy. Mater Sci Eng A. 2007;452–453:657-64.

20. Kostopoulos V, Baltopoulos A, Karapappas P, Vavouliotis A, Paipetis A. Impact and after-impact properties of carbon fibre reinforced composites enhanced with multiwall carbon nanotubes. Compos Sci Technol. 2010;70(4):553-63.

21. Santhosh MS, Sasikumar R, Natarajan E. E-Glass/phenolic matrix/APP laminate as a potential candidate for battery casing of e-vehicle - experimental investigations. Mater Res Express. 2021;8:045310.

22. Rahman M, Hosur M, Zainuddin S, Vaidya U, Tauhid A, Kumar A, et al. Effects of amino-functionalized MWCNTs on ballistic impact performance of E-glass/epoxy composites using a spherical projectile. Int J Impact Eng. 2013;57:108-18.

23. Nakatani H, Kosaka T, Osaka K, Sawada Y. Damage characterization of titanium/GFRP hybrid laminates subjected to low-velocity impact. Compos, Part A Appl Sci Manuf. 2011;42(7):772-81.

24. Li X, Zhang X, Zhang H, Yang J, Nia AB, Chai GB. Mechanical behaviors of Ti/CFRP/Ti laminates with different surface treatments of titanium sheets. Compos Struct. 2017;163:21-31.

25. Tarfaoui M, Lafdi K, El Moumen A. Mechanical properties of carbon nanotubes based polymer composites. Compos, Part B Eng. 2016;103:113-21.

26. Eslami-Farsani R, Aghamohammadi H, Khalili SMR, Ebrahimnezhad-Khaljiri H, Jalali H. Recent trend in developing advanced fiber metal laminates reinforced with nanoparticles: a review study. J Ind Text. 2020. In press.

27. Lee H, Lee J-G, Ryu J, Cho M. Twisted shape bi-stable structure of asymmetrically laminated CFRP composites. Composite Part B. 2017;108:345-53.

28. Zhang Z, Li Y, Wu H, Chen D, Yang J, Wu H, et al. Viscoelastic bistable behaviour of antisymmetric laminated composite shells with time-temperature dependent properties. Thin-walled Struct. 2018;122:403-15.

29. Yuan Z, Wang Y, Wang J, Wei S, Liu T, Cai Y, et al. A model on the curved shapes of unsymmetric laminates including tool-part interaction. Sci Eng Compos Mater. 2018;25(1):1-8.

30. Hu YB, Li HG, Cai L, Zhu JP, Pan L, Xu J, et al. Preparation and properties of fibre-metal laminates based on carbon fibre reinforced PMR polyimide. Compos, Part B Eng. 2015;69:587-91.

31. Natarajan E, Santhosh MS, Markandan K, Sasikumar R, Saravanakumar N, Dilip AA. Mechanical and wear behaviour of PEEK, PTFE and PU: review and experimental study. Journal of Polymer Engineering. 2022;42(5):407.

32. Moore M, Ziaei-Rad S, Salehi H. Thermal response and stability characteristics of bi-stable composite laminates by considering temperature dependent material properties and resin layers. Appl Compos Mater. 2013;20(1):87-106.